Circuit-Coupled FEM Analysis of the Electric-Field Type Intra-Body Communication Channel

Ruoyu Xu, Hongjie Zhu, and Jie Yuan
Department of Electronic and Computer Engineering
The Hong University of Science & Technology
Clear Water Bay, Kowloon, Hong Kong
Email: {xuruoyu, ee_zhxaa, eeyuan}@ust.hk

***Abstract*—The electric-field (EF) intra-body communication (IBC) is a promising data transmission method for high-speed low-power biomedical sensors. A good model of the EF-IBC channel is needed for better understanding the signal propagation principle and more efficient IBC transceiver design. Although various effective models have been developed for the waveguide IBC channel, the EF-IBC channel has only been modeled by empirical distributed RC network. In this paper, a circuit-coupled finite-element-method (FEM) model is established to analyze the EF-IBC channel. A multi-layer FEM model is developed for the human forearm. The parasitic effects of the probe PCBs and the return path are modeled as circuit elements. The circuit-coupled FEM model is simulated in ANSYS. Simulation results show that the model agrees well with the EF-IBC measurements. The circuit-coupled FEM model provides useful insights into the EF-IBC mechanism.**

I. INTRODUCTION

Personal health care requires wearable medical sensors to monitor patients continuously. Comfort and battery life time are two major issues in such applications. Intra-body communication (IBC) uses the human body as the signal transmission media. It removes the cumbersome wires and meanwhile has the potential to achieve lower power consumption than traditional wireless communication schemes [1].

There are two IBC methods: waveguide type [2][3][4] and electric-field (EF) type [5][6][7]. In waveguide IBC, a pair of transmitter (TX) electrodes imposes differential signals into the body and the body is used as a waveguide to propagate the signal. At the far end, the signal is detected by the receiver (RX) electrode pair. Waveguide IBC generally achieves low data rate in the kbps range because the body effectively shorts the TX electrodes.

The EF-IBC signal paths and the equivalent block diagram are shown in Fig. 1. Unlike waveguide IBC, only the signal electrodes of TX and RX are attached to the body in EF IBC. The ground (GND) planes of TX and RX are floated in the air. The body is used as the conductive forward path. The two floated GND planes are coupled to each other parasitically through the air and the external GND to close the signal loop.

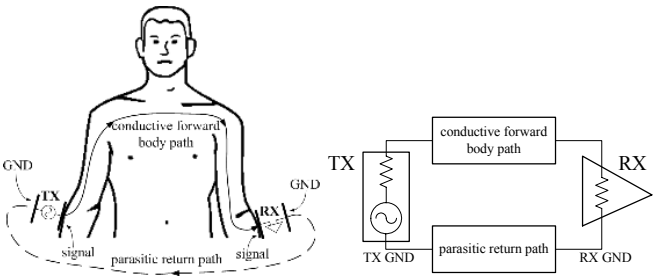

Fig. 1 EF-IBC system: (a) real model (b) block diagram

EF IBC can achieve higher data rate. Song *et al.* reported a 2-Mbps EF-IBC link in [7]. The high data rate is important in new medical sensory applications such as wireless capsule endoscopy [8] and neural recording [9].

Good models for IBC channels are being pursued by many researchers for better understanding the principles of the signal propagation. Moreover, the design of IBC transceiver can be much more robust and efficient with a good model.

The waveguide IBC channel has been modeled by simplified circuit, finite-element-method (FEM), finite-difference-time-domain (FDTD) method in [2], [3] and [4] respectively. The only model for EF IBC was based on the distributed RC network [6]. Also, parasitic effects of the probe PCBs were not considered, which undermines the EF-IBC model accuracy. Previously, our measurement showed that the EF-IBC channel attenuation has a bandpass profile which is mainly determined by the parasitic return path and the parasitics of the probe PCBs [10]. Therefore the parasitic effects of the probe PCBs must be considered in the model.

In this work, we developed a model mixed with FEM and circuits to analyze the EF-IBC channel. In the EF-IBC channel, the human forearm is modeled with FEM, while the probe PCBs and the return path are modeled by circuit elements. This circuit-coupled FEM model is simulated by ANSYS 11. The model enables us to investigate the potential distribution in different tissue layers. It also enables us to study the effects and parameters of different components in the EF-IBC channel. The EF-IBC channel attenuation is

978-1-4244-4918-7/09/$25.00 ©2009 IEEE

simulated based on the circuit-coupled FEM model and measured from 1 MHz to 100 MHz. The simulation results match the measurement data well.

II. Experiment Setup

S-parameters of the EF-IBC channel can be easily measured with a vector network analyzer (VNA). The channel attenuation is indicated by the forward transmission coefficient, S_{21}. A Rohde & Schwarz ZVB8 VNA is used for the measurement. As shown in Fig. 1(b), the EF-IBC channel consists of the conductive forward body path and the parasitic return path as well as the parasitics of the probe PCBs. To measure characteristics of different components in the EF-IBC channel, different experiment setup configurations are needed.

A. Probe PCBs

The probe PCBs are shown in Fig. 2(a). SMA A is connected to VNA ports. The 2cm×2cm copper foil is used as the signal electrode. It is connected to the signal strip at the front side of probe PCBs by a short wire. The characteristic impedance of the signal strip is designed as 50 Ω to match the cables. For SMA B, only the outer GND shield is used. It is soldered to the GND plane at the back side of probe PCBs. When the SMA B ports of TX and RX are connected by a cable, TX and RX share the same GND and the parasitic return path is shorted.

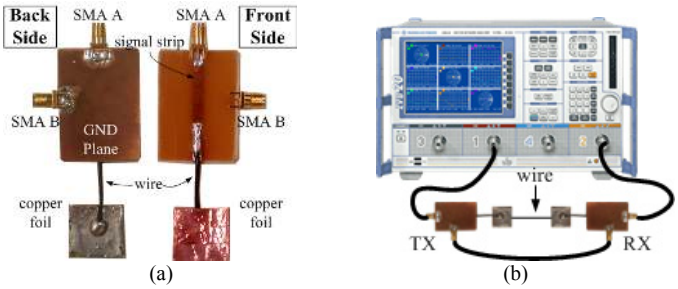

Fig. 2 Probe PCBs: (a) photographs (b) experiment setup

The experiment setup for probe PCBs is shown in Fig. 2(b). The signal electrodes of TX and RX are connected together with a wire. The SMA B ports are connected to each other with cable to eliminate the effect of the parasitic return path. Thus, parasitics of the PCB probes can be measured.

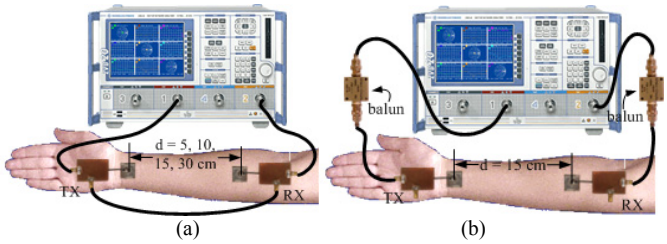

Fig. 3 Experiment setups for (a) conductive forward body path (b) complete EF-IBC channel

B. Conductive Forward Body Path

The experiment setup for conductive forward body path is shown in Fig. 3(a). The TX signal electrode is fixed at the wrist and the RX signal electrode can be moved at different positions on the forearm. The parasitic return path is shorted well.

C. Complete EF-IBC Channel

A complete EF-IBC channel needs the parasitic return path to close the signal loop. Since the ports of VNA share the same GND, the return path will be shorted if the SMA A ports of TX and RX are directly connected to VNA. As in the previous work [10], in the measurement setup of the complete EF-IBC channel, baluns are inserted between the probe PCB and the VNA port to preserve the parasitic return path, as shown in Fig. 3(b).

III. Circuit-Coupled FEM Model

To efficiently emulate the EF-IBC channel, components are modeled with different abstraction levels. A multi-layer FEM model is established for the human forearm. The parasitics of probe PCBs are modeled by LC circuits. The parasitic return path is also tentatively modeled by circuit elements.

A. FEM Model of Human Forearm

FEM model with concentric cylinders has been used to model the human upper arm in [3]. In this work, similar structure with different tissue and dimension parameters is applied for the human forearm. The multi-layer FEM model with electrodes is designed in ANSYS 11 as shown in Fig. 4 (a) and (b). The radius of the cylinder model is 40 mm. The model consists of 5 tissue layers: skin (1.2 mm), fat (6.8 mm), muscle (22 mm), cortical bone (4.8 mm) and bone marrow (5.2 mm). Different tissue layers are characterized by relative permittivity and conductivity. The parameters have been measured in [11] and shown in Fig. 5.

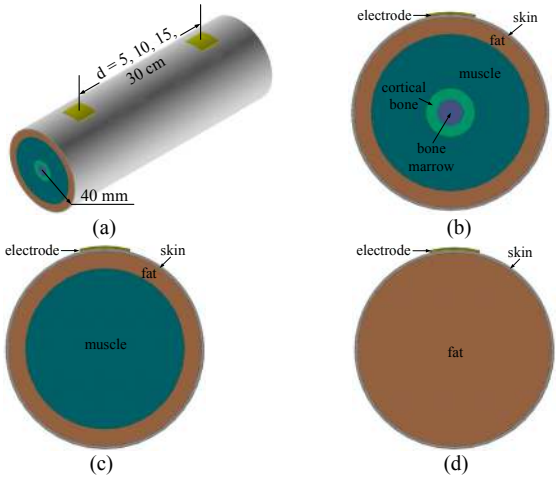

Fig. 4 FEM models of the human forearm: (a) 3-D view (b) cross section (c) without bone (d) without bone and muscle

The conductivity of every tissue increases with frequency. This results in lower body resistance with higher frequencies. Although the relative permittivity of every tissue decreases with rising frequency, the increasing frequency itself makes the equivalent body capacitive impedance smaller with high frequencies, as shown in Eq. (1). Therefore, the impedance of the human body decreases with rising frequency.

$$Z \downarrow = \frac{1}{j\omega C} = \frac{1}{j\omega \uparrow \frac{\varepsilon_0 \varepsilon_r \downarrow S}{d}} \tag{1}$$

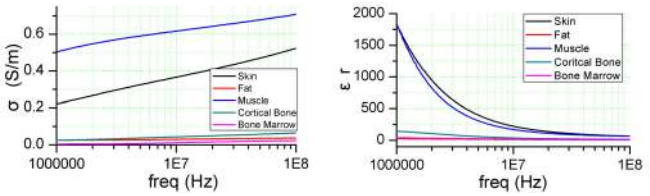

Fig. 5 Tissue parameters

To simulate the influence of different tissue layers on the channel characteristics, other two models are also made as shown in Fig. 4 (c) and (d). The model in Fig. 4(c) is composed of skin, fat and muscle. The model in Fig. 4(d) only includes skin and fat.

B. Model of Conductive Forward Body Path Measurement Setup

ANSYS 11 enables the circuit-coupled FEM simulation. The measurement setup for conductive forward body path in Fig. 3(a) can be modeled by the circuit-coupled FEM model in Fig. 6(a). The probe PCB parasitics are modeled by capacitors and inductors with values extracted from the probe PCBs measurement. The source and load impedance (50 Ω) of the equipment are also added in the model.

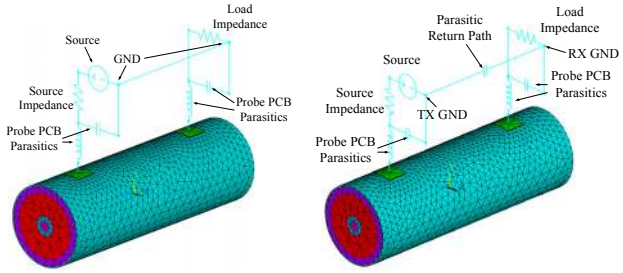

(a) (b)

Fig. 6 Circuit-coupled FEM models: (a) conductive forward body path (b) complete EF-IBC channel

C. Model of the Complete EF-IBC Channel Measurement Setup

The parasitic return path is usually considered as a capacitive path between the GNDs of TX and RX. In this work, a capacitor is added between the GNDs of TX and RX of the previous circuit-coupled FEM model to emulate the measurement setup of the complete EF-IBC channel as shown in Fig. 6(b). As the capacitance of the return path can not be easily estimated from measurement results, different values are used in simulations for better estimation.

IV. RESULTS AND ANALYSES

A. Probe PCBs

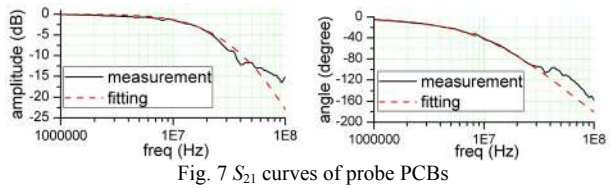

Fig. 7 S_{21} curves of probe PCBs

The measured S_{21} curves of the probe PCBs are shown in Fig. 7. It has a first-order lowpass profile. The probe PCB can be modeled by an inductor in the signal line and a capacitor between the signal and GND lines. Simulation with this LC model agrees with the measurements well as shown in Fig. 7, both in amplitude and phase. The inductance and the capacitance are 550 nH and 35 pF respectively. According to the microwave theory, these parasitics are caused by the discontinuity of the micro-strip line on probe PCBs [12]. The parasitics tend to block the signal propagation at high frequencies.

B. Conductive Forward Body Path

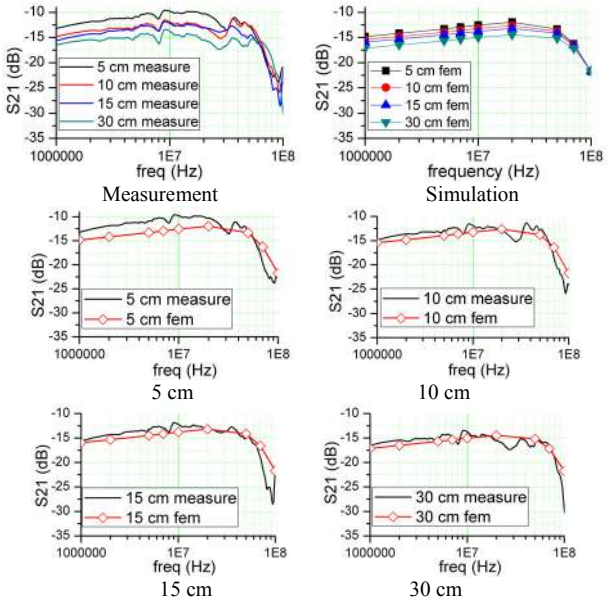

Fig. 8 Measured and simulated S_{21} curves for conductive forward body path

The measurement and simulation results for the conductive forward body path (Fig. 3(a) and Fig. 6(a)) are shown in Fig. 8 with different distances (d = 5, 10, 15, 30 cm) between TX and RX. Larger distance leads to higher attenuation. When the frequency increases from 1 MHz, S_{21} rises slightly at all distances. It results from the decreasing human impedance. When the frequency reaches 50 MHz, S_{21} curves drop rapidly. This is caused by the lowpass feature of the probe PCBs, which outweighs the decreasing body impedance. As shown in Fig. 10, the large deviation of the simulated S_{21} curve when d = 15 cm without the probe PCB circuit model indicates that the parasitics of probe PCBs cannot be ignored.

When the distance between TX and RX is 5 cm, the measured S_{21} is about 2 dB higher than the simulated one, as shown in Fig. 8. It is probably caused by the direct capacitive coupling between TX and RX signal electrodes. The coupling creates an additional forward path to improve the signal propagation. At larger distances, the impedance of this additional forward path becomes much larger than the body so that the forward path is dominated by the body. Therefore the simulation results match the measured data better at larger distances.

The potential distributions in the forearm FEM model with d = 15 cm are shown in Fig. 9. The equipotential lines concentrate in the shallow layers, namely skin, fat and muscle. The simulated S_{21} with the other two forearm FEM models in Fig. 4 (c) and (d) are plotted in Fig. 10. Without bone, the simulated EF-IBC channel does not change much. However, the simulated S_{21} deviates from the measurements a lot when

the muscle is removed. Therefore, the conductive forward path is mainly formed by the surface layers, which includes skin, fat and muscle. The bone layer can be removed to reduce the model complexity without degrading the simulation accuracy.

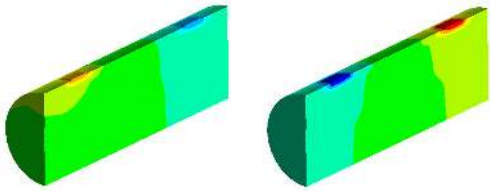

Real Part Imaginary Part

Fig. 9 Potential distributions in the forearm FEM model

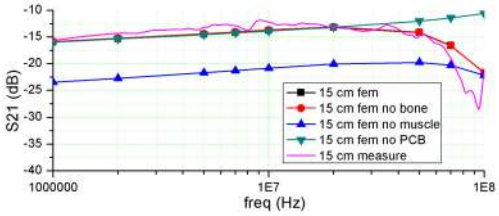

Fig. 10 Simulated S_{21} curves without bone, muscle or PCBs

C. *Complete EF-IBC Channel*

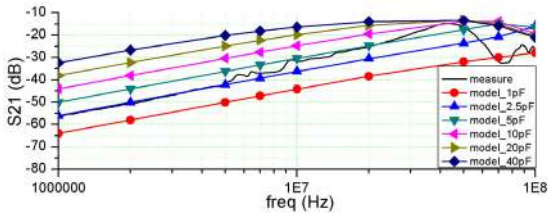

Fig. 11 S_{21} curves of the complete EF-IBC channel

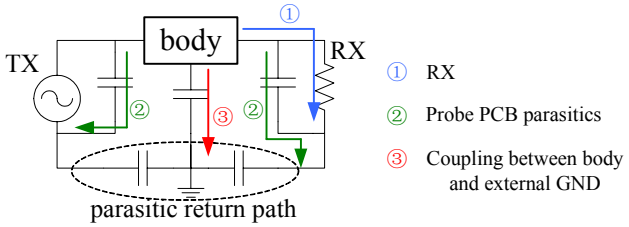

Fig. 12 Signal flows in the complete EF-IBC Channel

6 different capacitance values are used for the parasitic return path. The measured and simulated S_{21} curves of the complete EF-IBC channel with d = 15 cm are plotted in Fig. 11. Simulations on the circuit-coupled FEM model are able to generate the typical bandpass profile of the EF-IBC channel. However, the simulated curves can not perfectly match the measured EF-IBC channel profile. Nonetheless, the simulation can provide useful insights into the EF-IBC channel. The rising slope of the measured S_{21} curve lies between simulated curves with 2.5-pF and 10-pF return path capacitance. This indicates the capacitance of the parasitic return path is frequency dependent. Its value varies from 2.5 to 10 pF below 40 MHz. The falling slope of the measured S_{21} curve is much steeper than the simulation results. This indicates that besides the parasitic shunt path of the probe PCBs, there exist other factors to shunt the signal from propagating to RX at high frequencies. This could be due to the coupling between the body and the external GND as shown in Fig. 12, which is also frequency dependent.

V. CONCLUSION

In this paper, a circuit-coupled FEM model has been established for the EF-IBC channel. A multi-layer FEM model is developed for the human forearm. Parasitics of the probe PCBs are modeled by circuit elements. The values of the circuit elements are extracted from the measurement results. The simulation results of the circuit-coupled FEM conductive forward body path match the measurement results well. FEM simulation results reveal that the signal propagation occurs mainly in the surface layers of the body such as skin, fat and muscle. Simulation results of the circuit-coupled FEM complete EF-IBC channel indicate that the capacitance of the parasitic return path is frequency dependent. Its value varies in the range from 2.5 to 10 pF. The coupling between the body and the external ground will also shunt the signal at high frequencies. Overall, the circuit-coupled FEM modeling approach provides valuable insights into mechanism of the EF-IBC channel, and offers reasonably good accuracy for the design of EF-IBC system.

REFERENCES

[1] J. A. Ruiz, Jiang Xu and S. Shimamoto, "Propagation characteristics of intra-body communications for body area networks," Consumer Communications and Networking Conference, 2006. CCNC 2006. 3rd IEEE, vol. 1, pp. 509-513, 2006.

[2] K. Hachisuka, Y. Terauchi, Y. Kishi, T. Hirota, K. Sasaki, H. Hosaka and K. Ito, "Simplified circuit modeling and fabrication of intrabody communication devices," Solid-State Sensors, Actuators and Microsystems, 2005. Digest of Technical Papers. TRANSDUCERS '05. the 13th International Conference on, vol. 1, pp. 461-464 Vol. 1, 2005.

[3] M. S. Wegmueller, A. Kuhn, J. Froehlich, M. Oberle, N. Felber, N. Kuster and W. Fichtner, "An attempt to model the human body as a communication channel," IEEE Transactions on Biomedical Engineering, vol. 54, pp. 1851-1857, 2007.

[4] K. Fujii, M. Takahashi and K. Ito, "Electric Field Distributions of Wearable Devices Using the Human Body as a Transmission Channel," Antennas and Propagation, IEEE Transactions on, vol. 55, pp. 2080-2087, 2007.

[5] T. G. Zimmerman, "Personal area networks: Near-field intrabody communication," IBM Systems Journal, vol. 35, pp. 609-617, 1996.

[6] N. Cho, J. Yoo, S. -. Song, J. Lee, S. Jeon and H. -. Yoo, "The Human Body Characteristics as a Signal Transmission Medium for Intrabody Communication," Microwave Theory and Techniques, IEEE Transactions on, vol. 55, pp. 1080-1086, 2007.

[7] Seong-Jun Song, Namjun Cho and Hoi-Jun Yoo, "A 0.2-mW 2-Mb/s Digital Transceiver Based on Wideband Signaling for Human Body Communications," Solid-State Circuits, IEEE Journal of, vol. 42, pp. 2021-2033, 2007.

[8] H. Chan, and J. Yuan, "Current-Mode Temporal Difference CMOS Imager for Capsule Endoscopy", 2007 IEEE Biomedical Circuits and Systems Conference(BioCAS), pp. 219-222, Montreal, Canada, Nov. 27-30, 2007.

[9] C. Chestek, P. Samsukha, M. Tabib-Azar, R. Harrison, H. Chiel, and S. Garverick, "Microcontroller-based wireless recording unit for neurodynamic studies in saltwater", IEEE Sensors J., Vo. 6, pp. 1105-1114, Oct. 2006.

[10] R. Xu, H. Zhu, J. Yuan, "Characterization and Analysis of Intra-body Communication Channel", 2009 IEEE International Symposium on Antennas and Propagation (APS), accepted.

[11] S.Gabriel, R.W.Lau and C.Gabriel: "The dielectric properties of biological tissues: III. Parametric models for the dielectric spectrum of tissues", Phys. Med. Biol. 41 (1996), 2271-2293.

[12] D. M. Pozar, Microwave Engineering. ,3rd ed.Hoboken, NJ: John Wiley & Sons, 2005, pp. 700.